Handheld sensing system for data-driven irrigation management in olive orchards

Eliseo Roma,[1] Francisco Rovira-Más,[2] Pietro Catania[1]

[1]Department of Agricultural, Food and Forest Sciences, University of Palermo, Italy; [2]Department of Rural and Agrifood Engineering, Polytechnic University of Valencia, Spain

Abstract

Proper water management is necessary to optimize the quantity and quality of olive oil. The advent of monitoring tools capable of providing reliable and systematic information on tree water status, and thus vegetative growth, can be advantageous for growers of olive groves. Leaf temperature, environmental conditions, crop water stress index (CWSI), and other related vegetation indices (VI) measured non-invasively using proximal sensing tools are being increasingly employed for agriculture 4.0 applications. This study aimed to implement and evaluate a low-cost handheld system to determine the water conditions of olive trees under different irrigation treatments. Implementation of the data-driven system required the selection of the most efficient CWSI equation for the developed proximal sensing device. Specifically, five potential equations were evaluated, including two analytical models, one empirical equation derived from existing literature, a newly proposed empirical equation, and a hybrid model combining analytical and empirical calculations. The sensing system was equipped with a Global Navigation Satellite System (GNSS), an infrared thermometer, a compact NDVI sensor with ambient light correction, and an environmental measuring unit providing air temperature and relative humidity. Additionally, the leaf water potential (LWP) was calculated in real time to better determine the actual hydric stress conditions of the trees. All data were acquired between 12:00 and 14:00 on both the sunny and shaded canopy sides. The experimental results showed that the handheld system eased the collection of field data to help growers schedule and manage irrigation for olive oil production through stress identification and precise GPS positioning. The best correlation between LWP and CWSI was found for the analytical formulas ($R^2 = 0.62$), followed by the empirical formula ($R^2 = 0.55$); however, both analytical equations required a higher number of measurements when compared to the alternative models considered, which complicated their practical implementation in the handheld prototype.

Correspondence: Eliseo Roma, Department of Agricultural, Food and Forest Sciences, University of Palermo, viale delle Scienze, Ed. 4, 90128 Palermo, Italy. E-mail: eliseo.roma@unipa.it

Key words: CWSI; irrigation management; NDVI; proximal sensing; smart farming; water stress.

Contributions: ER, FRM, PC, conceptualization, investigation, methodology, manuscript review and editing; ER, FRM, data curation; ER, formal analysis; FRM, PC, validation, supervision; ER, PC, manuscript original drafting. All authors read and approved the final version of the manuscript and agreed to be accountable for all aspects of the work.

Conflict of interest: the authors declare no known competing financial interests that could have appeared to influence the work reported in this paper.

Funding: no funds, grants, or other support was received.

Acknowledgments: this work was supported by the project "Piattaforma DIGItale per La difesa di precisione dell'OliVEto" – "DIGILOVE",- "National Research Centre for Agricultural Technologies (Agritech)" (MUR, PNRR-M4C2, CN00000022), Spoke 2 'Università degli Studi di Napoli Federico II', CUP: E63C22000920005.
The authors are grateful to the Agricultural Robotics Laboratory research group of the Polytechnic University of Valencia for the scientific collaboration and personal support, in particular to: Dr. V. Saiz-Rubio, Prof. E. Ortiz, Mr. A. Cuenca Cuenca, Mr. Montano Pérez, Prof. A. Torregrosa, and Prof. C. Ortiz.

Received: 17 January 2024.
Accepted: 29 September 205.

Journal of Agricultural Engineering 2025; LVI:1960
doi:10.4081/jae.2025.1960

Introduction

The optimization of irrigation management for specialty crops is one of the main resources to increase production efficiency. In the last thirty years, olive growing has undergone a continuous change in cultivation techniques due to new types of planting (Tous *et al*. 2010). Although olive trees tolerate water stress well, the correct water supply can lead to higher yields and quality (Fernández *et al*., 2018; Tognetti *et al*., 2006) because the amount of water supplied can determine vegetative growth, plant yield (Roma *et al*., 2023), and even the amount of polyphenols (Caruso *et al*., 2014, 2019). In olive orchards, efficient water management strategies try to maintain slight to moderate stress levels or even induce stress during specific phenological stages to optimize both yields and high-quality oil. To accomplish this, accurate, regular, and reliable measurements of crop water status are crucial to ensure a predetermined level of stress. At present, there exist various methods for assessing water stress conditions in orchards,

either from remote or proximal sensing platforms equipped with sensors providing measurements on the trees or their surrounding atmosphere (Roma and Catania, 2022; Sghaier *et al*., 2022; Vanella *et al*., 2021). The temperature of the leaves and canopies strongly depends on the transpiration rate, and therefore it can be used as an indicator of stomatal opening and indirectly of tree stress. The potential of monitoring canopy temperature to detect stress has been reported for various crops (Allen *et al*., 1998; Bellvert *et al*., 2014; Liang, 2004; Testi *et al*., 2008). Specifically, the stomatal closure induced by water stress reduces the transpiration rate, decreasing evaporative cooling and thus increasing leaf temperature, which can be monitored using infrared thermometers and thermal cameras. This approach to detecting water stress became very popular in the 1970s and 1980s with the advent of portable thermometers. Clawson and Blad (1982), for instance, proposed canopy temperature variability as an index of water stress, and Oerke *et al.* (2011, 2006) used leaf temperature as an indicator for disease detection. The practical tracking of canopy temperature T_c uses the difference between the minimal and maximal T_c known as the critical temperature variability (CTV; Clawson and Blad, 1982) or the standard deviation of T_c (σ_{Tc}) within the canopy (González-Dugo *et al.,* 2012), which first increases with mild stress in almond trees and then decreases again under more severely stressed vegetation. Despite the initial good results found with these methods, their dependence on weather and specific crop characteristics results in practical limitations. As a result, there is still a need to develop further normalized indices to overcome the effects of those unpredictable environmental parameters that influence the relationship between plant stress and canopy temperature. To date, the most popular crop stress index is the crop water stress index (CWSI), initially developed by Idso *et al.* (1981) and Jackson *et al.* (1981). This index is an indicator of drought stress that utilizes the temperatures of a dry crop, and a crop that transpires at its maximum rate (λE_{pot}), characterized by its canopy resistance (rc_{pot}) and temperature (T_{pot}). On the other hand, the dry crop, with associated λE_{dry}, rc_{dry}, and T_{dry}, represents an identical crop that does not transpire. Therefore, the CWSI is determined by Equation (1):

$$CWSI = 1 - \frac{\lambda E}{\lambda E_{pot}} = \frac{\Delta T_{pot} - \Delta T}{\Delta T_{pot} - \Delta T_{dry}} = \frac{(T_{pot} - T_a)_{LL} - (T_c - T_a)}{(T_{pot} - T_a)_{LL} - (T_{dry} - T_a)_{UL}} \quad \text{(Eq. 1)}$$

where: ΔT_{pot}, ΔT_{dry}, and ΔT are respectively defined as $(T_{pot} - T_a)_{LL}$, $(T_{dry} - T_a)_{UL}$, and $(T_c - T_a)$; the UL (upper limit) and LL (lower limit) thresholds indicate the minimum and maximum transpiration rates of plants.

In Eq. (1), ΔT denotes the measured canopy-air temperature difference, ΔT_{pot} is the lower limit equivalent to a canopy transpiring at the potential rate, and ΔT_{dry} is the non-transpiring canopy. According to this definition, when a canopy is transpiring at its potential rate, CWSI is 0 (no stress), and likewise, when the canopy is not transpiring, CWSI = 1 (high stress). This simple normalization requires that T_{dry} and T_{pot} are known. Several theoretical formulations have been proposed to determine the CWSI (Maes and Steppe, 2012), such as the analytical method ($CWSI_A$), the empirical solution ($CWSI_E$), the direct approach ($CWSI_D$), and a hybrid solution that simplifies the calculation equation.

The analytical approach requires the measurement of incoming solar radiation, air temperature, relative humidity, wind speed and vegetative data (average canopy height and leaf length). These environmental variables can be obtained from a conventional meteorological station, and can be representative for the entire orchard; however, there is often uncertainty in the estimation of canopy resistances, which complicates the practical implementation of this approach (Jackson et *al*., 1981). In particular, two analytic equations have been developed to estimate T_{pot}. The first equation (2) was proposed by Jackson *et al.* (1981) to calculate T_{pot} setting the canopy resistance ($r_c = 0$), where R_n is the net radiative flux density (W m^{-2}), ρ is the air density (kg m^{-3}), C_p is the specific heat at constant pressure (J kg^{-1} $^{\circ}K^{-1}$), γ is the psychrometric constant (Pa $^{\circ}K^{-1}$), Δ is the slope of the saturated vapor pressure *vs* temperature curve (Pa $^{\circ}K^{-1}$) and can be calculated according to Eqs. 3 or 3.1 (T_m is the average between canopy and air temperature), r_a is the aerodynamic resistance (s m^{-1}), e^* is the saturated vapor pressure of the air (Pa) at canopy temperature (Tc), and e is the vapor pressure of the air (Pa).

$$T_{pot} = T_{air} + \frac{r_a * Rn}{\rho C_p} * \frac{\gamma}{\Delta+\gamma} - \frac{e^* - e}{\Delta+\gamma} \quad \text{(Eq. 2)}$$

$$\Delta = \frac{e^* - e}{T_c - T_a} \quad \text{(Eq. 3)}$$

$$\Delta = 45.03 + 3.014 * T_m + 0.05345 * T_m^2 + 0.00224 * T_m^3 \quad \text{(Eq. 3.1)}$$

Although the previous method is occasionally applied in research, current studies determine ΔT_{pot} with an alternative equation that rearranges the basic energy balance to estimate the canopy resistance directly from water vapor transfer (Ben-Gal *et al*., 2009; Li *et al*., 2010). Specifically, the theoretical temperatures T_{pot} and T_{dry} can be calculated with Eq. (4) and (5) respectively, where Rn_i is the isothermal net radiative flux density (W m^{-2}), VPD is the vapor pressure deficit (kPa), Δ is the slope of saturated water vapor pressure *versus* temperature curve (kPa $^{\circ}K^{-1}$), γ is the psychrometric constant (kPa K^{-1}), ρ is the air density (kg m^{-3}), C_p is the specific heat at constant pressure (J kg^{-1} $^{\circ}K^{-1}$), r_w is the total resistance to vapor transports (s m^{-1}), and r_{HR} is the resistance to heat and radiative transport (Facchi *et al*., 2013; Jones, 1992, 1999; Monteith, 1973).

$$T_{pot} = T_{air} - \frac{r_{HR}\, r_w\, \gamma}{\rho C_p (\Delta\, r_{HR} + r_w\, \gamma)} Rn_i + \frac{r_{HR}}{\Delta\, r_{HR} + r_w\, \gamma} VPD \quad \text{(Eq. 4)}$$

$$T_{dry} = T_{air} + \frac{Rn_i\, r_{HR}}{\rho C_p} \quad \text{(Eq. 5)}$$

In the analytic method, T_{dry} is obtained when the leaf does not transpire, and all the available energies dissipate into sensible heat. In reality, both analytic methods are essentially the same, and require several standard meteorological data (T_{air}, VPD, R_n, wind speed) and the estimation of other parameters such as the roughness length of momentum (z_{0M}), the zero-displacement height (d) and the canopy height (h_c).

The empirical method ($CSWI_E$) was proposed by Idso *et al.* (1981) based on the strong correlation between ΔT (T_c-T_a) and the VPD. Idso *et al.* (1981, 1982) demonstrated that the lower limit of the CWSI is a linear function of VPD for a number of crops and locations. As a result, the equation to determine the upper and lower limits are different (Jones, 1992); the No-Water-Stress-Baseline (NWSB) represents a fully watered crop (lower limits, LL), whereas the maximum stressed baseline (upper limits, UL) corresponds to a non-transpiring crop. These baselines can be calculated from the following equations, where the VP_{sat} (T_a) is the saturation vapor pressure at air temperature, and VP_{sat} (T_a+a) is the

saturation vapor pressure at air temperature plus the intercept value a for the crop of interest (Jones, 2013):

$$\Delta T_{ll} = \alpha + \beta * VPD \quad \text{(Eq. 6)}$$

$$\Delta T_{ul} = \alpha + \beta\left(VP_{sat}(T_a) - VP_{sat}(T_a + \alpha)\right) \quad \text{(Eq. 7)}$$

Notice, however, that the slope b and intercept a have been determined only for a limited number of crops, with only two available studies having calculated both coefficients for olive orchards (Berni *et al.*, 2009; Egea *et al.,* 2017). The basic assumption of this method is that a and b are constant and crop-specific, at least for a given location and for a certain growth stage. To simplify the calculation of T_{dry} in both the analytical and empirical methods, an additional calculation method has been proposed (Cohen *et al.*, 2005; Jones *et al.*, 2002; Möller *et al.*, 2007), according to the following formula:

$$T_{dry5} = T_a + 5°C \quad \text{(Eq. 8)}$$

The last approach to obtain the CWSI is the direct method ($CWSI_D$), where T_{pot} and T_{dry} are directly obtained in the field. T_{pot} is equivalent to T_c for a fully transpiring plant, and similarly, T_{dry} can be estimated by measuring canopy temperature in a no transpiring plant. T_{pot} is generally obtained by spraying a thin layer of water on one or both leaf sides before each measurement. Alternatively, T_{dry} is induced by covering canopy leaves with a layer of petroleum jelly, blocking thus all transpiration flows. This method has been applied in a limited number of studies with good results (Maes *et al*., 2011; Wang *et al*., 2010). However, despite the promising prospects for the direct method, it is not widely applied due to the need for frequent calibrations and the lack of consistency of satisfactory results. Additionally, no previous experiences, to the authors' knowledge, have been reported on the application of the direct method to olive trees. In spite of the difficulties posed by the direct method for its practical implementation in the field, the method has risen the interest of remote sensing (Sepulcre-Cantó *et al.*, 2006). For such applications, to calculate the CWSI for each pixel, it is important to have two temperature references, the wet-bulb reference equivalent to T_{pot}, and the dry-bulb reference corresponding to T_{dry} (Bastiaanssen *et al.*, 1998; Möller *et al.*, 2007; Veysi *et al.*, 2017).

The number of methods described above, and developed in previous decades, demonstrate the benefits of having access to monitoring tools capable of providing accurate information regarding water status in olive groves, mainly those offering high temporal and spatial resolution. However, orchard growers also demand portable and user-friendly tools that can be easily employed for irrigation scheduling (Gardner *et al.*, 1992; Yuan *et al.*, 2004). In recent years, the number of ground-based thermal monitoring in orchards has increased significantly. There are two reasons for this increased interest. First, the application of thermal cameras from the ground allows for the precise assessment of T_c with an easier removal of noise from the soil and background. Second, the availability of more ground data brings more reliable information to understand real water status at tree level, even though the sensors of the 1990s were only capable of detecting low variability. Nowadays, cost-efficient sensors can be easily integrated with various technologies to deliver accurate results that can be seamlessly incorporated into the geographic information systems (GIS), but handy handheld systems have not yet been extensively developed and tested for spectral monitoring of water and other relevant olive orchard conditions.

The aim of this research was to implement and evaluate a customized handheld system equipped with multiple sensors to detect water stress conditions in olive trees, and objectively assist in irrigation management. The decision-making algorithm embedded in the system focused on a reformulation of the CWSI and the influence of vegetative vigor from NDVI to determine the water stress levels.

Materials and Methods

Study area

The field experiments were carried out in a research plot located in Valencia, Spain (Figure 1).

The climate of the area where the experimental plot is located is Mediterranean, with an average annual rainfall lower than 500 mm, concentrated from autumn to spring. According to the Koppen-Geiger classification, the climate of the area is classified

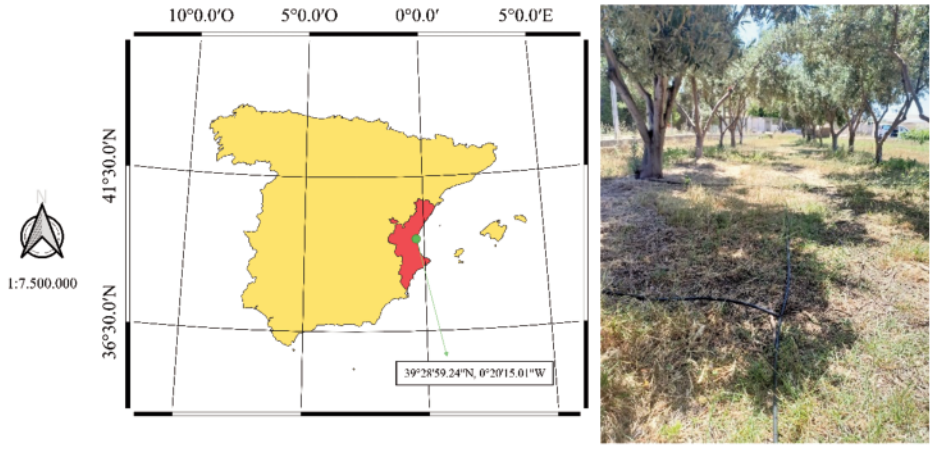

Figure 1. Location of the experimental plot.

as Mediterranean hot summer (Kottek *et al.*, 2006). The soil moisture regime is xeric, border with aridic, and the temperature regime is thermic. The main characteristics of the soil particles, according to the ISSS (International Society of Soil Science), is sandy clay (Hillel, 2013). The trials were carried out in 20 olive trees (*Olea europaea* subsp. *europaea*) monitored along the 2022 season. The plantation layout was rectangular with row spacing of 4.5 m and plant spacing of 4 m in a NE-SO direction. At the time of the trial, the plants were in full productivity, with good vigor conditions and a height between 3 m and 5 m.

Experimental design

The experimental design involved two irrigation treatments: full irrigation (FI) and deficit irrigation (DI). In DI, the rain was the only supply of water to the trees, whereas in FI, the supply of water followed the needs of evapotranspiration calculated with the Penman-Monteith equation (Allen *et al.*, 1998). Specifically, the irrigation volumes were calculated using the crop evapotranspiration (ET_c) of Eq. (8), where the reference evapotranspiration (ET_0) was calculated with the FAO-Penman-Monteith method (Allen *et al*., 1998), the crop coefficient (K_c) was 0.55 for conventional olive trees, and the coefficient of ground cover (K_r) was 0.46.

$$ET_c = ET_o \cdot K_c \cdot K_r \quad \text{(Eq. 9)}$$

Once the evapotranspiration was calculated, a hydrological balance was estimated to schedule irrigation. Of the 20 plants monitored, 9 were subjected to F) and the remaining 11 to DI. FI trees were irrigated using a surface drip irrigation system, with a separation of 0.75 m between emitters discharging 8 L x h^{-1}. Figure 2 shows the layout of the irrigation system used for the experiments.

Handheld monitoring system

The handheld monitoring system was embedded in the functional prototypes of Figure 3, designed and built at the Agricultural Robotics Laboratory of the Polytechnic University of Valencia (Spain). The devices have a trigger to capture data points with all the embedded sensors, including a GPS receiver to enable site-specific rapid monitoring. The system runs on a rechargeable Li-ion battery of 7.4 VDC and capacity of 2.6 Ah, capable of feeding all the sensors, a processor, and a TFT-LCD screen of 1.8" that shows the details of the measurements being taken. The sensing capacity of the device used in these experiments with olive trees is divided into three sub-systems: positioning, crop data, and environmental data. The positioning sub-system consists of a GPS receiver NEO-6 (U-Blox, Thalwil, Switzerland) working at 5 Hz and with a precision of approximately 2.5 m. The crop sensing subsystem comprises an infrared thermometer (Melexis, Ypres, Belgium) to measure canopy temperature and a spectral reflectance sensor (Apogee, Logan, UT, USA) to estimate the NDVI with a field of view of 36° and a correction sensor for ambient illumination. Finally, the environmental subsystem includes a low voltage temperature sensor TMP36 (One Technology Way, Norwood, MA, USA) to track air temperature around the device, and a humidity sensor HIH 4000 (Honeywell, Charlotte, NC, USA) to sense relative humidity.

Data acquisition in the field

Field data were collected during the 2022 season for the 20 olive trees under evaluation. Before the beginning of the experiments, each tree was georeferenced with a GPS receiver (Stonex, Monza, Italy). All measurements were executed at midday, from 12:00 to 14:00, to determine the LWP and the CWSI at the most critical time of the day. The LWP was measured as the ground truth validation for the models, and required three shoot samples from the bright side of the canopy. Each shoot comprised several leaves, which were carefully inserted into a Scholander pressure chamber (PWSC 3000; Soil Moisture Equipment Corp., Goleta, CA, USA) following standard procedures (Moriana *et al.*, 2012; Sepulcre-Cantó *et al.*, 2006). The temperature of the canopy (T_c) was measured near the samples selected for LWP validation for the bright sides, and additionally in the shaded side of the canopy. The acquisition angle at which the handheld device was oriented was 60° from the zenith axis (Huband and Monteith 1986), with the purpose of eliminating the influence of the soil and the sunlight (Chehbouni *et al.*, 2001; Jones *et al.*, 2003), and at a distance of 1 meter from the olive tree.

The calculation of the CWSI with the analytic method requires the additional measurements of wind speed and net solar radiation, neither of which was available from the handheld prototype. As a result, a Kestrel 5400 datalogger (Nielsen-Kellerman Company, Boothwyn, PA, USA) positioned 2 m above the ground was mounted to provide the missing parameters net radiation and wind speed. The handheld device was equipped with a GPS receiver to provide global positioning, and therefore site-specific monitoring. The positioning accuracy of the embedded receiver was evaluated by comparing positions measured with the S7 Stonex receiver as a reference in three different locations within the Valencia province under different weather conditions: sunny, cloudy and overcast. The S7 Stonex was already described in previous studies (Catania *et al.*, 2020, 2021).

Application of CWSI equations

This study required the application of the $CWSI_A$ analytic model based on Equations 2 and 4, and the application of the $CWSI_E$ empirical model, with the purpose of avoiding the poor results in olives found from other models such as that of Berni *et al.* (2009) and Egea *et al.* (2017).

Calculation of parameters for the application of the analytic model $CWSI_A$

The analytic method requires the estimation of T_c, meteorological data, and the set of parameters described as follows. The leaf boundary layer resistance to heat transfer (r_H) can be estimated with equation 9 (Guilioni *et al*., 2008), where d (m) is the leaf length in the direction of the wind, and u (m s^{-1}) is the wind speed at the height of the leaf, usually estimated from a wind profile.

$$r_H = 100\sqrt{\frac{d}{u}} \quad \text{(Eq. 10)}$$

The leaf resistance to radiative transfer (r_R) can be rewritten as eq. 10 (Guilioni *et al.*, 2008), where ε_L is the emissivity of the leaf, σ is the Stefan-Boltzmann constant (5.67×10^{-8} Wm^{-2} K^{-1}), ρ is the density of air, C_p is the specific heat of air at constant pressure, and T_a is the air temperature.

$$r_{HR} = \frac{r_H r_R}{(r_H + r_R)} \quad \text{(Eq. 11)}$$

Finally, the total resistance to heat and radiative transfer r_{HR} is

given by eq. 12.

$$r_R = \frac{\rho C_p}{(8\,\varepsilon_l\,\sigma\,T_a^3)} \quad \text{(Eq. 12)}$$

Generally speaking, leaves exchange heat and water vapor with the surrounding air through their both sides. The leaf resistance to transfer water vapour ($\mathbf{r_W}$) was calculated from leaf temperature T_c and environmental variables, on the basis of a linearized form of the standard energy balance equation (Guilioni *et al.*, 2008; Jones, 1992). However, the transpiration for the olive tree mostly occurs in the lower side of the leaf (known as hypostomatous leaves), and therefore another method was deemed more appropriate. In particular, the r_W was calculated from Eq. 13, where r_{s2} is the stomatal resistance only in the lower side and $\mathbf{r_{aWl}}$ is the boundary layer resistance to water vapor transport. Notice that r_{aWl} is slightly lower than the coefficient for sensible heat, as explained by Jones (1992) and specified as: $r_{aWl} = 0.92 \times r_H$.

$$r_W = r_{S2} + r_{aWl} \quad \text{(Eq. 13)}$$

To apply equation 2, the potential canopy resistance ($\mathbf{r_{cp}}$) was evaluated with Eq. 13 (Agam *et al.*, 2013; Moriana and Fereres, 2002; Testi *et al.*, 2006), where $\mathbf{r_a}$ is the aerodynamic resistance and the stomal resistance was considered to be the resistance of the canopy.

$$r_{cp} = \frac{r_a(e_c^* - e_a)}{\gamma\left(\frac{r_a\,Rn}{\rho\,c_p} - (T_c - T_a)\right)} \quad \text{(Eq. 14)}$$

The parameter $\mathbf{r_a}$ is difficult to calculate as it requires multiple parameters. They can be estimated with drag partition models, taking canopy height ($\mathbf{h_c}$, m), width (m), and element spacing into account (Raupach, 1992). This research used two equations (Eq. 15 and Eq. 16) because they had shown good results in previous studies and can be used for different wind speed conditions (Maes and Steppe, 2012; Thom and Oliver, 1977). Precisely, Eq. 15 was used under 2 m s^{-1} wind speed and Eq. 16 was applied for higher values. The effective aerodynamic resistance ($\mathbf{r_{ae}}$) includes the influence of buoyancy on aerodynamic resistance, and was calculated with the Thom and Oliver (1977) empirical method of Eq. 15,where **z** (m) is the reference height , **u** is the wind speed (m s^{-1}), **d** (m) is the zero-displacement height, **k** is the constant of Karman (0.41), and $\mathbf{z_{0M}}$ (m) is the roughness length of momentum. The displacement height d and roughness length z_{0M} are complex functions of the vegetation height and architecture, which were estimated as d =0.732*h_c and z_0 = 0.113*h_c according to Berni *et al.* (2009).

$$r_{ae} = 4.72\,\frac{[\ln(\frac{z-d}{z_{0M}})]^2}{(1+0.54\,u)} \quad \text{(Eq. 15)}$$

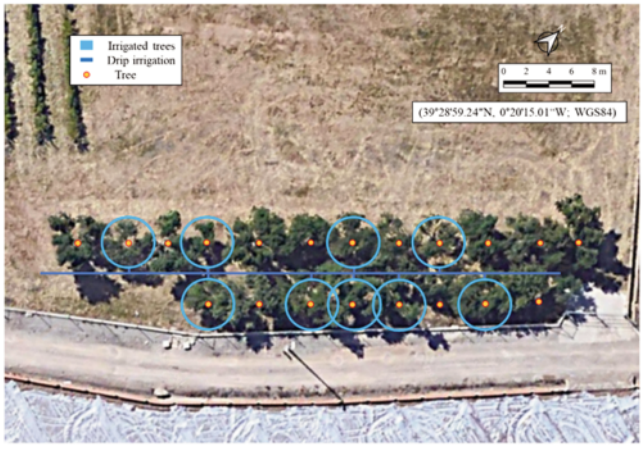

Figure 2. Experimentation site and irrigation design.

Figure 3. Handheld prototypes for rapid assessment of tree stress.

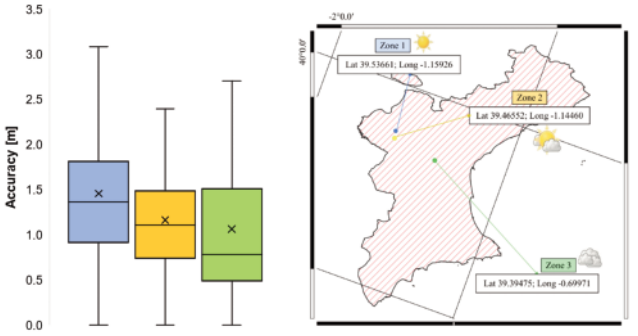

Figure 4. Comparison among locations and weather conditions for GPS accuracy.

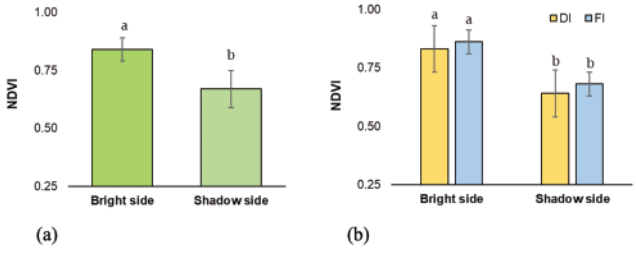

Figure 5. NDVI results. **a**) Comparison between sunny and shaded sides of the canopy. **b**) Comparison between irrigation treatments.

$$r_a = \frac{\left\{ln\frac{[(z-d)]}{z_0}\right\}^2}{k\,u} \quad \text{(Eq. 16)}$$

An alternative approach to obtain r_{cp} was also considered according to O'Toole and Real (1986), as detailed in equations 17 and 18, where the coefficients α and β were determined from previous research (Berni *et al.* 2009; Egea *et al.* 2017) and our own experience.

$$r_{ap} = \frac{\rho\, C_p\, \alpha}{R_n\, \beta\, (\Delta + \frac{1}{\beta})} \quad \text{(Eq. 17)}$$

$$r_{cp} = -r_{ap}\left[\frac{\Delta + 1/\beta}{\gamma} + 1\right] \quad \text{(Eq. 18)}$$

Calculation of parameters for the application of the empirical model CWSI$_e$

The empirical method was developed by Idso (1982), and its application requires T_a, VPD and T_c as inputs. Specifically, ΔT_{pot} was obtained with equation 6 and our own coefficients α and β, whereas T_{dry} was calculated with equations 7 and 8 widely used in the specialized literature.

Results

The tests envisioned to challenge the accuracy of the positioning receiver embedded in the handheld device revealed that the low-cost system was able to maintain a positioning error under 2 m, even in harsh weather conditions. The ANOVA test (Figure 4) shows that there were no statically significant differences in accuracy among the locations and weather conditions.

The spectral profile of the tree canopy was satisfactorily registered by the handheld instrument of Figure 3. NDVI measurements collected from both canopy sides showed values of 0.84±0.05 for the sunny side, and 0.67±0.08 for the shaded side, according to the ANOVA test of Figure 5, which confirmed that leaves in the bright side have higher values of NDVI than in the shaded side, with statically significant differences at p<0.001. However, no statistical differences were observed for the irrigation treatments (Figure 5b).

The average environmental conditions at which the tests were carried out were 31.8°C for the air temperature, 50% for relative humidity, 2 m/s for wind speed, and 980 W/ m^2 for the net solar radiation. All parameters were used to determine the lower and upper limits for canopy temperature and the resulting CWSI, as detailed in Table 1.

The comparison among CWSI models to assess hydric stress yielded similar trends and behavior. The canopy temperature depended on irrigation. The stress indicator based on the CWSI$_A$ showed small differences when compared to the ground-truth validation assessed with the LWP (Figure 6). As expected, the LWP

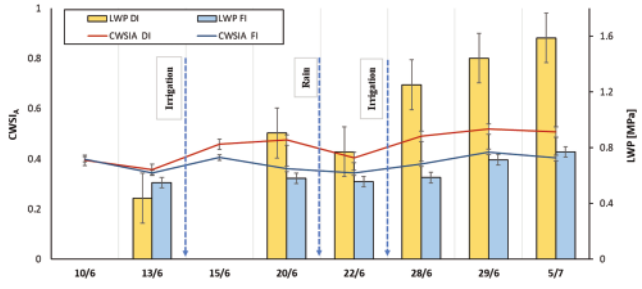

Figure 6. Comparison of stress indicators LWP and CWSIa during the experimentation period.

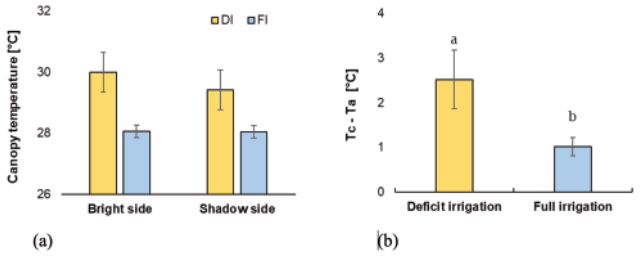

Figure 7. Analysis of canopy temperature. **a)** Interaction between irrigation treatments and canopy side. **b)** ΔT for each irrigation treatment.

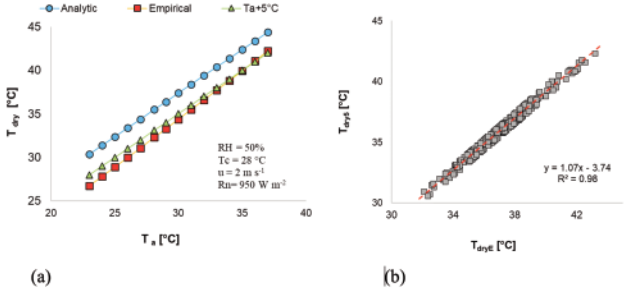

Figure 8. **a)** Different T_{dry} obtained with the analytic and empirical equations (5, 7 and 8). **b)** Relationship between T_{dryE} (Eq. 7) and T_{dry5} (Eq. 8).

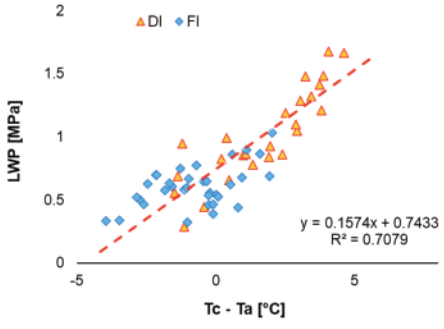

Figure 9. Correlation between the leaf water potential directly estimated with a pressure chamber and the difference of temperatures (ΔT) for both irrigation treatments. The squares indicate the data obtained from the FI treatment, while the triangles are derived from the DI treatment.

measured in the deficitary trees (DI) doubled the magnitude of LWP in irrigated trees, divergences that were not corroborated by the analytical models. The canopy temperature (T_c) of each tree was not only related to its water status, but also to soil-plant-environment interactions. The results showed that the canopy side did not influence canopy temperature consistently, as there were no statistically significant differences between the canopy temperature for the FI treatment, although higher T_c values were measured in the deficitary trees for both sides, as expected and plotted in Figure 7a. The two-way ANOVA of Figure 7a showed that the irrigation treatment influenced the canopy temperature (p<0.001), and there was not side effect. In general, ΔT was lower in FI trees than in DI trees, as plotted in Figure 7b, with statically significant differences confirmed by an ANOVA test (p<0.001).

The upper (T_{dry}) and lower (T_{pot}) limits for the canopy temperature were obtained through different approaches. The upper temperature (T_{dry}) kept similar values and showed a good correlation with the analytic and empirical methods described above (Figure 8a). The best correlation was observed between the direct calculation T_{dry5} and the empirical T_{dryE} calculated with Eqs. 8 and 7, with an R^2 of 0.98 (Figure 8b). The lowest correlation was found between analytical T_{dryA} (Eq. 5) and T_{dry5} (Eq. 8) with an R^2 of 0.75.

The lower canopy temperature limit (T_{pot}) was observed for the trees under the FI treatment, with good correlations and statically significance among the considered approaches. The best correlations to detect water stress were found between DT and LWP, with an R^2 of 0.71 as plotted in Figure 9. The LWP measurements carried out with the Scholander chamber on sampled shoots differed for the two irrigation programs implemented, being always under 2 MPa, which in general indicates moderate levels of stress. In particular, the LWP for DI conditions had an average of 1.2±0.46 MPa, whereas in the FI system was 0.63±0.2.

Water stress has been well correlated to vapor pressure deficit (VPD) for several crops (Bellvert *et al.,* 2014; Testi *et al.,* 2008; Veysi *et al.,* 2017), as the transpiration of plants is physiologically related to the VPD of the atmosphere. For the case of olive trees, such correlation held according to the results plotted in Figure 9. The NWBL represents the line that correlates DT and VPD under optimal water conditions (Idso *et al.,* 1981), and as indicated in Figure 10, showed a strong correlation with the VPD (R^2 = 0.81).

The goal of this research is to establish a methodology to calculate CWSI from non-invasive measurements, with the final objective of easing automation in irrigation scheduling. The implementation of the empirical model ($CWSI_E$) led to a strong linear relationship with various parameters and resulted a good predictor of tree water status. The coefficients that were empirically determined in our experiments were β=1.885 and α=-0.398. $CWSI_E$ was able to differentiate the hydrologic status of the plants under the two irrigation treatments (Figure 11).

The analytical models $CWSI_J$ and $CWSI_A$ yielded the best results, with no statistical differences between the two calculation metFIhods. The difference between $CWSI_J$ and $CWSI_A$ is in the method to obtain T_{pot}; in $CWSI_J$ is obtained with Eq. 2 whereas in $CWSI_A$ with Eq. 4. Both $CWSI_J$ and $CWSI_A$ showed a strong relationship with LWP, with statistical significance determined by an R^2 of 0.62 and 0.57 as represented in Figure 12. As expected, the two irrigation treatments yielded differentiated CWSI values, where the FI trees reached lower values and less linearity than the DI trees.

Alternatively, when the $CWSI_j$ was calculated with the coefficients α and β to obtain T_{pot}, the results were not satisfactory. However, the introduction of our own coefficients led to better results than the use of the coefficients reported by Berni *et al.* (2009) and Egea *et al.* (2017). In addition to the correlation with the LWP, both $CWSI_j$ and $CWSI_A$ showed a good relationship with

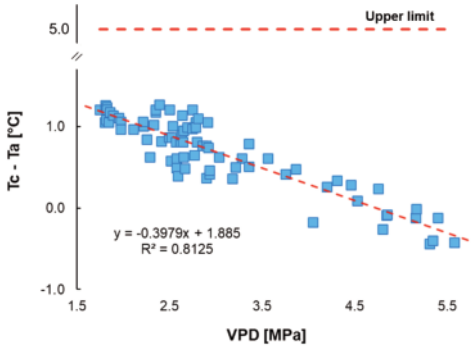

Figure 10. Representation of the No-Water-Stress-Baseline obtained in the experimental site.

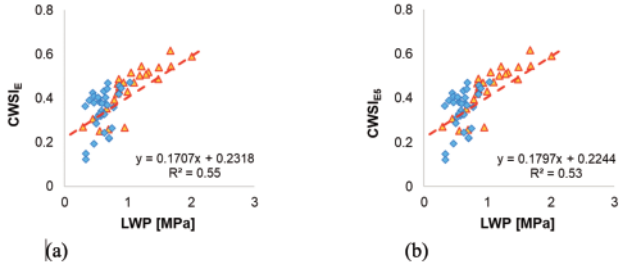

Figure 11. a) Correlation between $CWSI_E$ and the LWP using Eqs. 6 and 7 to obtain the lower and upper limits. b) Correlation between $CWSI_{E5}$ and LWP using Eqs. 6 and 8 to obtain the lower and upper limits. The squares indicate the data obtained from the full irrigation treatment, while the triangles are derived from the deficit irrigation treatment.

Table 1. Main parameters used to calculate the CWSI with Eqs. 4 and 5.

CWSIA	Tpot	Tdry	RH	Rn	Tc	Ta	u	e	VPD	Δ	rHR	ra	rW
-	°C	°C	%	W m^{-2}	°C	°C	m s^{-1}	kPa	kPa		s m-1	s m^{-1}	s m^{-1}
0.62	20.02	32.85	70	950	28	26	2	3.36	1.01	209.19	26.34	8.87	24.23
0.53	21.28	33.85	70	950	28	27	2	3.56	1.07	214.53	25.82	8.87	23.75
0.35	23.79	35.85	70	950	28	29	2	4.00	1.20	225.69	24.73	8.87	22.76
0.25	25.04	36.85	70	950	28	30	2	4.24	1.27	231.51	24.17	8.87	22.24

DT, as shown in Figure 13, which is an excellent finding because DT (T_c-T_a) is a parameter readily available with the device of Figure 3.

Discussion

This research provided an overall framework for estimating the actual water potential of olive trees with the use of low-cost handheld systems for irrigation management. The low-cost GNSS receiver demonstrated sufficient accuracy for tree positioning in several weather conditions, as errors stayed below 2 m in olive groves where canopy dimensions are often above 4 m and row spacing typically reaches 6-8 m. These results emphasize the role that low-cost positioning systems can play in spreading the use of smart technologies in agriculture, even though low-cost receivers do not achieve the same positioning accuracy as the survey-grade ones (Jackson *et al*., 2018). Low-cost receivers can achieve cm-level accuracy when using high quality antennas to reduce the influence of weather conditions (Karaim *et al*., 2018). The handheld system of Figure 3 facilitates importing field-collected data onto GIS platforms.

The NDVI differences found per canopy side confirm previous studies (Catania *et al*., 2023); different sun radiation levels for each canopy side influenced the growth of the trees. In general, sunny sides were more vigorous, as estimated by the NDVI data.

The hydric status of the two sides of the canopy also exhibited different behaviors. The temperature difference DT was less negative in irrigated trees, whereas trees in stressed conditions tended to have higher values, as observed in previous studies (Egea *et al*., 2017; Sepulcre-Cantó *et al*., 2006). Although DT was strongly correlated with LWP, its measurement cannot be directly used for irrigation management because it is not a direct indicator of water conditions (Fernández *et al*., 2018). As hypothesized by Clawson and Blad (1982), the variability of thermal conditions between different canopy zones is distinct within each plant. Our study revealed less variability in T_c data for well-irrigated plants (FI). In coincidence with González-Dugo *et al.* (2012), trees under D) showed greater variability and higher canopy temperatures, what evidences the important role played by thermal dynamics for irrigation management.

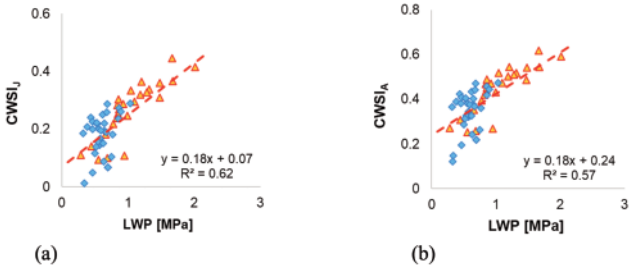

Figure 12. Correlation between analytical models for the CWSI and the LWP. **a)** CWSIJ. **b)** CWSIA. The squares indicate the data obtained from the FI treatment, while the triangles are derived from the Di treatment.

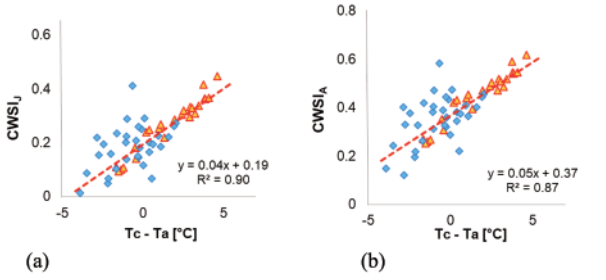

Figure 13. Correlation between the analytical expressions of CWSI and ΔT. **a)** CWSIJ. **b)** CWSIA. The squares indicate the data obtained from the FI treatment, while the triangles are derived from the DI treatment.

Optimizing the quantity and quality of olive oil requires accurate water management. The increase of irrigation volumes up to a certain level enhances yield; however, a certain degree of stress can improve the quality of oil. As a result, it is important to have monitoring tools capable of providing precise information on water status of olive groves. This research has shown the benefits of portable systems to provide accurate data on tree health status and assist in irrigation management for olive production. The field experiments validated the use of the CWSI calculated with different methodologies when compared to the ground truth measurements of the LWP, in agreement with Bellvert *et al.* (2016) for peaches and Egea *et al*. (2017) for olives. Ben-Gal *et al.* (2009) also observed a high correlation of the CWSI with the soil water content (SWC). In the comparison among several CWSI models, Agam *et al*. (2013) observed better results for the empirical formulation than for analytical formulas, although results are not comparable with the present study because T_{pot} was obtained from a wet object. Contrarily, Ben-Gal *et al.* (2009) tested $CWSI_A$ and $CWSI_E$ methods in an olive orchard with irrigation treatments and found both methods to perform well, with no statistically significant differences between them. Despite the fact that the Jackson method has been proven to be the most accurate, it has not been as widely applied (Berni *et al.,* 2009; Jackson *et al.*, 1981; Li *et al*., 2010; Yuan *et al*., 2004) as the $CWSI_A$ formulation, which has provided satisfactory results on various crops to discriminate well-watered trees (Jones, 1992, 1999, 2013).

Although this study is in line with Ben-Gal *et al*. (2009) and Berni *et al*. (2009), $CWSI_j$ yielded the best results; however, the amount of data required complicates its implementation in handheld instruments. One reason for that is that it needs more environmental variables than Idso's model (Idso, 1982), such as the crop resistances at potential transpiration. In fact, there were no significant differences between the two analytical formulas implemented, but the $CWSI_A$ has a simpler formulation as there is no need to calculate certain parameters that are difficult to derive, and no estimation of rc_{pot} as formulated by O'Toole and Real (1986) has been found for olive trees. This approach results from an empirical approximation of the analytical method for obtaining T_{pot} (Jackson *et al*., 1981), which relies on well-calibrated alpha and beta coefficients.

Among the main limitations associated with the empirical $CWSI_E$, is worth mentioning the widespread use of T_{dry5} as the reference value for the stressed baseline in different crops (Irmak *et al*., 2000; Möller *et al*., 2007), including olive trees (Agam *et al*., 2013; Ben-Gal *et al*., 2009), given that various studies have demonstrated the high sensitivity of $CWSI_E$ to T_{dry} (Cohen *et al*., 2005; Irmak *et al*., 2000; Möller *et al*., 2007). Our study confirmed that the utilization of T_{dry5} does not significantly alter the results compared to using T_{dryE} or T_{dryA}, although choosing the appropriate T_{dry} can further reduce uncertainty. Interestingly, the NWBL obtained was different from the equations determined by Berni *et*

al. (2009) and Egea *et al*. (2017) for olive orchards. These differences were probably due to their different climatic and cultivation conditions. Specifically, the formula found (NWBL = 1.88 - 0.398 x VPD) showed larger dispersion and smaller slope compared with baselines reported for other crops; indeed, large variations of VPD resulted in small differences of ΔT when compared to herbaceous and some tree species such as pistachio (Testi *et al*., 2008) due to the high capacity of olive leaves to regulate the transpiration rate (Moriana *et al*., 2002; Villalobos *et al*., 2006).

Conclusions

The considerable number of publications using the difference of canopy-air temperature to estimate tree stress would suggest that abundant data exists to validate the theoretical approach. Unfortunately, most papers miss key parameters such as net radiation, wind speed, or air temperature near the evaluated canopy. The difficulty of measuring all the necessary parameters to apply the theoretical approaches is the reason for the simplicity of the empirical approaches.

The research reported in this article confirmed that the CWSI can be calculated with different methodologies, and all the models tested were valid for irrigation management because they were closely related to LWP, which was the variable chosen as ground-truth. In general, both analytic and empirical CWSI showed satisfactory results, but the calculation of analytic CWSI needs the measurement of more environmental variables than the $CWSI_E$, which discards it for handheld instruments. The $CWSI_E$, on the contrary, is a valid substitute for the $CWSI_j$ and $CWSI_A$ in the detection of water stress as long as field calibrations are made. Overall, the developed handheld system was a helpful tool for the tree-specific detection of water stress, but also of instantaneous crop conditions, as it evaluated the different spectral profiles of the two sides of the canopy, as well as differences in canopy temperature, underlining the importance of monitoring canopy development to better manage water stress conditions.

The overall conclusion of this research is the proof that the conventional water stress index CWSI can be implemented in non-invasive systems, which in turns enables the automated assessment of tree water status at high spatial precision and sensing accuracy. Such crucial properties for precision farming were attained by merging a cost-effective GNSS receiver with proximal sensing sensors that closely monitor the surrounding environment of individual trees, something that is out of reach for non-terrestrial platforms. At present, the LWP is the only standard method for the general assessment of water stress, but the cumbersome handling of Scholander chambers has limited their use exclusively for research, leaving field managers in olive groves without practical tools for handling crop stress and canopy growth. This paper is an initiative to start changing the current situation and help promoting the real deployment of precision agriculture concepts within Mediterranean crops.

References

Agam, N., Cohen, Y., Berni, J., Alchanatis, V., Kool, D., Dag, A., et al. 2013. An insight to the performance of crop water stress index for olive trees. Agric. Water Manag. 118:79–86.

Allen, R.G., Pereira, L.S., Raes, D., Smith, M. 1998. Crop evapotranspiration-Guidelines for computing crop water requirements-FAO Irrigation and drainage paper 56. Fao, Rome. Available from: https://www.fao.org/4/x0490e/x0490e00.htm

Bastiaanssen, W.G., Menenti, M., Feddes, R., Holtslag, A. 1998. A remote sensing surface energy balance algorithm for land (SEBAL). 1. Formulation. J. Hydrol. 212:198–212.

Bellvert, J., Marsal, J., Girona, J., Gonzalez-Dugo, V., Fereres, E., Ustin, S.L., Zarco-Tejada, P.J. 2016. Airborne thermal imagery to detect the seasonal evolution of crop water status in peach, nectarine and Saturn peach orchards. Remote Sens. 8:39.

Bellvert, J., Zarco-Tejada, P. J., Girona, J., Fereres, E. 2014. Mapping crop water stress index in a 'Pinot-noir'vineyard: comparing ground measurements with thermal remote sensing imagery from an unmanned aerial vehicle. Precis. Agric. 15:361-376.

Ben-Gal, A., Agam, N., Alchanatis, V., Cohen, Y., Yermiyahu, U., Zipori, I., et al. 2009. Evaluating water stress in irrigated olives: correlation of soil water status, tree water status, and thermal imagery. Irrig. Sci. 27:367-376.

Berni, J., Zarco-Tejada, P., Sepulcre-Cantó, G., Fereres, E., Villalobos, F. 2009. Mapping canopy conductance and CWSI in olive orchards using high resolution thermal remote sensing imagery. Remote Sens. Environ. 113:2380-2388.

Caruso, G., Gucci, R., Urbani, S., Esposto, S., Taticchi, A., Di Maio, I., et al. 2014. Effect of different irrigation volumes during fruit development on quality of virgin olive oil of cv. Frantoio. Agric. Water Manag. 134:94–103.

Caruso, G., Palai, G., D'onofrio, C., Gucci, R. 2019. Sustainable management of water and soil in olive orchards and vineyards under climate change. Agrochimica 2019:125-132.

Catania, P., Orlando, S., Roma, E., Vallone, M. 2021. Vineyard design supported by GPS application. Acta Hortic. 1314:227-234.

Catania, P., Comparetti, A., Febo, P., Morello, G., Orlando, S., Roma, E., Vallone, M. 2020. Positioning accuracy comparison of GNSS receivers used for mapping and guidance of agricultural machines. Agronomy 10:924.

Catania, P., Roma, E., Orlando, S., Vallone, M. 2023. Evaluation of multispectral data acquired from UAV platform in olive orchard. Horticulturae 9:133.

Chehbouni, A., Nouvellon, Y., Lhomme, J.-P., Watts, C., Boulet, G., Kerr, Y., et al. 2001. Estimation of surface sensible heat flux using dual angle observations of radiative surface temperature. Agric. For. Meteorol. 108:55–65.

Clawson, K.L., Blad, B.L. 1982. Infrared thermometry for scheduling irrigation of corn 1. Agron. J. 74:311–316.

Cohen, Y., Alchanatis, V., Meron, M., Saranga, Y., Tsipris, J. 2005. Estimation of leaf water potential by thermal imagery and spatial analysis. J. Exp. Bot. 56:1843–1852.

Egea, G., Padilla-Díaz, C.M., Martinez-Guanter, J., Fernández, J.E., Pérez-Ruiz, M. 2017. Assessing a crop water stress index derived from aerial thermal imaging and infrared thermometry in super-high density olive orchards. Agric. Water Manag. 187:210-221.

Facchi, A., Gharsallah, O., Gandolfi, C. 2013. Evapotranspiration models for a maize agro-ecosystem in irrigated and rainfed conditions. J. Agric. Eng. 44:411.

Fernández, J.E., Diaz-Espejo, A., Romero, R., Hernandez-Santana, V., García, J.M., Padilla-Díaz, C.M., Cuevas, M.V. 2018. Precision irrigation in olive (Olea europaea L.) tree orchards. In: I.F. Garcia Tejero, V.H. Duran Zuazo (eds.), Water scarcity and sustainable agriculture in semiarid environment. Cambridge, Academic Press. pp. 179–217.

Gardner, B., Nielsen, D., Shock, C. 1992. Infrared thermometry

and the crop water stress index. I. History, theory, and baselines. J. Prod. Agr. 5:462–466.
Gonzalez-Dugo, V., Zarco-Tejada, P., Berni, J.A., Suarez, L., Goldhamer, D., Fereres, E. 2012. Almond tree canopy temperature reveals intra-crown variability that is water stress-dependent. Agric. For. Meteorol. 154:156-165.
Guilioni, L., Jones, H., Leinonen, I., Lhomme, J.-P. 2008. On the relationships between stomatal resistance and leaf temperatures in thermography. Agric. For. Meteorol. 148:1908–1912.
Hillel, D. 2013. Fundamentals of soil physics. Cambridge, Academic Press.
Huband, N., Monteith, J. 1986. Radiative surface temperature and energy balance of a wheat canopy. Bound. Layer Meteorol. 36:1-17.
Idso, S.B. 1982. Non-water-stressed baselines: a key to measuring and interpreting plant water stress. Agric. Meteorol. 27:59–70.
Idso, S., Jackson, R., Pinter Jr, P., Reginato, R., Hatfield, J. 1981. Normalizing the stress-degree-day parameter for environmental variability. Agric. Meteorol. 24:45–55.
Irmak, S., Haman, D.Z., Bastug, R. 2000. Determination of crop water stress index for irrigation timing and yield estimation of corn. Agron. J. 92:1221–1227.
Jackson, J., Saborio, R., Ghazanfar, S.A., Gebre-Egziabher, D., Davis, B. 2018. Evaluation of low-cost, centimeter-level accuracy OEM GNSS receivers. Report Number: MN/RC 2018-10. Available from: https://rosap.ntl.bts.gov/view/dot/35402
Jackson, R.D., Idso, S., Reginato, R., Pinter Jr, P. 1981. Canopy temperature as a crop water stress indicator. Water Resour. Res. 17:1133–1138.
Jones, H.G. 1992. Plants and microclimate: a quantitative approach to environmental plant physiology. Cambridge, Cambridge University Press.
Jones, H.G. 1999. Use of infrared thermometry for estimation of stomatal conductance as a possible aid to irrigation scheduling. Agric. For. Meteorol. 95:139–149.
Jones, H.G. 2013. Plants and microclimate: a quantitative approach to environmental plant physiology. Cambridge, Cambridge University Press.
Jones, H.G., Archer, N., Rotenberg, E., Casa, R. 2003. Radiation measurement for plant ecophysiology. J. Exp. Bot. 54:879–889.
Jones, H.G., Stoll, M., Santos, T., de Sousa, C., Chaves, M.M., Grant, O.M. 2002. Use of infrared thermography for monitoring stomatal closure in the field: application to grapevine. J. Exp. Bot. 53:2249–2260.
Karaim, M., Elsheikh, M., Noureldin, A., Rustamov, R. 2018. GNSS error sources. In: R.B. Rustamov, A.M. Hashimov (eds.), Multifunctional operation and application of GPS. IntechOpen. pp. 69–85.
Kottek, M., Grieser, J., Beck, C., Rudolf, B., Rubel, F. 2006. World map of the Köppen-Geiger climate classification updated. Meteorol. Z. 15:259-263.
Li, L., Nielsen, D., Yu, Q., Ma, L., Ahuja, L. 2010. Evaluating the crop water stress index and its correlation with latent heat and CO2 fluxes over winter wheat and maize in the North China plain. Agric. Water Manag. 97:1146–1155.
Liang, S. 2004. Quantitative remote sensing of land surfaces. Hoboken, Wiley.
Maes, W., Steppe, K. 2012. Estimating evapotranspiration and drought stress with ground-based thermal remote sensing in agriculture: a review. J. Exp. Bot. 63:4671-4712.
Maes, W.H., Achten, W., Reubens, B., Muys, B. 2011. Monitoring stomatal conductance of Jatropha curcas seedlings under different levels of water shortage with infrared thermography. Agric. For. Meteorol. 151:554-564.
Möller, M., Alchanatis, V., Cohen, Y., Meron, M., Tsipris, J., Naor, A., et al. 2007. Use of thermal and visible imagery for estimating crop water status of irrigated grapevine. J. Exp. Bot. 58:827–838.
Monteith, J. 1973. Principles of environmental physics. London, Edward Arnold.
Moriana, A., Fereres, E. 2002. Plant indicators for scheduling irrigation of young olive trees. Irrig. Sci. 21:83–90.
Moriana, A., Pérez-López, D., Prieto, M., Ramírez-Santa-Pau, M., Pérez-Rodriguez, J. 2012. Midday stem water potential as a useful tool for estimating irrigation requirements in olive trees. Agric. Water Manag. 112:43–54.
Moriana, A., Villalobos, F., Fereres, E. 2002. Stomatal and photosynthetic responses of olive (Olea europaea L.) leaves to water deficits. Plant Cell Environ. 25:395–405.
Oerke, E-C, Fröhling, P., Steiner, U. 2011. Thermographic assessment of scab disease on apple leaves. Precis. Agric. 12:699–715.
Oerke, E-C., Steiner, U., Dehne, H.-W., Lindenthal, M. 2006. Thermal imaging of cucumber leaves affected by downy mildew and environmental conditions. J. Exp. Bot. 57:2121–2132.
O'Toole, J., Real, J. 1986. Estimation of aerodynamic and crop resistances from canopy temperature 1. Agron. J. 78:305–310.
Raupach, M. 1992. Drag and drag partition on rough surfaces. Bound. Layer Meteorol. 60:375–395.
Roma, E., Catania, P. 2022. Precision oliviculture: research topics, challenges, and opportunities - A review. Remote Sens. 14:1668.
Roma, E., Laudicina, V.A., Vallone, M., Catania, P. 2023. Application of precision agriculture for the sustainable management of fertilization in olive groves. Agronomy 13:324.
Sepulcre-Cantó, G., Zarco-Tejada, P.J., Jiménez-Muñoz, J., Sobrino, J., De Miguel, E., Villalobos, F.J. 2006. Detection of water stress in an olive orchard with thermal remote sensing imagery. Agric. For. Meteorol. 136:31–44.
Sghaier, A., Dhaou, H., Jarray, L., Abaab, Z., Sekrafi, A., Ouessar, M. 2022. Assessment of drought stress in arid olive groves using HidroMORE model. J. Agric. Eng. 53:1264.
Testi, L., Goldhamer, D., Iniesta, F., Salinas, M. 2008. Crop water stress index is a sensitive water stress indicator in pistachio trees. Irrig. Sci. 26:395–405.
Testi, L., Orgaz, F., Villalobos, F.J. 2006. Variations in bulk canopy conductance of an irrigated olive (Olea europaea L.) orchard. Environ. Exp. Bot. 55:15–28.
Thom, A., Oliver, H.R. 1977. On Penman's equation for estimating regional evaporation. Q. J. R. Meteorol. Soc. 103:345–357.
Tognetti, R., d'Andria, R., Lavini, A., Morelli, G. 2006. The effect of deficit irrigation on crop yield and vegetative development of Olea europaea L.(cvs. Frantoio and Leccino). Eur. J. Agron. 25:356–364.
Tous, J., Hermoso, J., Romero, A. 2010. New trends in olive orchard design for continuous mechanical harvesting. Adv. Hort. Sci. 24:43:52
Vanella, D., Ferlito, F., Torrisi, B., Giuffrida, A., Pappalardo, S., Saitta, D., et al. 2021. Long-term monitoring of deficit irrigation regimes on citrus orchards in Sicily. J. Agric. Eng. 52:1193.
Veysi, S., Naseri, A.A., Hamzeh, S., Bartholomeus, H. 2017. A satellite based crop water stress index for irrigation scheduling in sugarcane fields. Agric. Water Manag. 189:70–86.

Villalobos, F., Testi, L., Hidalgo, J., Pastor, M., Orgaz, F. 2006. Modelling potential growth and yield of olive (Olea europaea L.) canopies. Eur. J. Agron. 24:296–303.

Wang, X., Yang, W., Wheaton, A., Cooley, N., Moran, B. 2010. Automated canopy temperature estimation via infrared thermography: A first step towards automated plant water stress monitoring. Comput. Electron. Agr. 73:74-83.

Yuan, G., Luo, Y., Sun, X., Tang, D. 2004. Evaluation of a crop water stress index for detecting water stress in winter wheat in the North China Plain. Agric. Water Manag. 64:29–40.